Contribution from the Department of Chemistry,
Massachusetts Institute of Technology, Cambridge, Massachusetts 02139

Synthesis, Structure Determination, and Electronic Structure Characterization of Two Mixed-Valence Tetranuclear Platinum Blues with Bridging α-Pyridonate or 1-Methyluracilate Ligands

Thomas V. O'Halloran, Pradip K. Mascharak, Ian D. Williams, Michael M. Roberts, and Stephen J. Lippard*

Received September 18, 1986

The second and third tetranuclear mixed-valence platinum(2.25+) blues to be characterized crystallographically are reported. The compound $[(en)Pt(C_5H_4NO)_2Pt(en)]_2(NO_3)_5 \cdot H_2O$ (**1**), where en = ethylenediamine and C_5H_5NO is α-pyridonate, crystallizes in triclinic space group $P\bar{1}$, $Z = 1$, with $a = 10.652$ (1) Å, $b = 13.068$ (2) Å, $c = 9.413$ (1) Å, $\alpha = 108.65$ (2)°, $\beta = 96.63$ (1)°, $\gamma = 68.39$ (1)°, and $V = 1157.1$ Å^3. The *cis*-diammineplatinum 1-methyluracilate ($C_5H_5N_2O_2$) analogue $[(H_3N)_2Pt(C_5H_5N_2O_2)_2Pt(NH_3)_2]_2(NO_3)_5 \cdot 5H_2O$ (**2**) also crystallizes in $P\bar{1}$, $Z = 2$, with $a = 10.123$ (3) Å, $b = 13.084$ (4) Å, $c = 19.508$ (7) Å, $\alpha = 92.28$ (3)°, $\beta = 101.09$ (3)°, $\gamma = 107.49$ (2)°, and $V = 2405.2$ Å^3. The Pt–Pt bond lengths in **1**, 2.830 (1) and 2.916 (1) Å for the outer and inner pairs of platinum atoms in the linear, zigzag chain, are longer by 0.06 and 0.04 Å, respectively, than comparable distances in *cis*-diammineplatinum α-pyridone blue, $[(H_3N)_2Pt(C_5H_4NO)_2Pt(NH_3)_2]_2(NO_3)_5 \cdot H_2O$ (**3**), owing to nonbonded interactions between ethylenediamine chelate rings in adjacent platinum coordination planes. The Pt–Pt distances in **2** are values intermediate between those in **1** and **3**. A semiquantitative model based on previous SCF–Xα calculations for **3** is used to correlate energy changes in the visible absorption bands of these three mixed-valence $(Pt^{2.25})_4$ blues with their Pt–Pt distances. Moreover, the lowest energy visible band of **1**–**3** can be qualitatively rationalized by a model in which the unpaired electron is delocalized in a one-dimensional box, the length of which is determined by the end-to-end Pt–Pt distance in the chain. Magnetic susceptibility studies have also been carried out which establish that **1** and **2** have $S = {}^1/_2$ ground states, with $\mu_{eff} = 1.94$ and 1.89 μ_B, respectively.

Introduction

The reactions of platinum(II) ammine complexes with purines, pyrimidines, and related heterocyclic amides have been extensively studied since the discovery of the antitumor activity of *cis*-diamminedichloroplatinum(II)[1] (*cis*-DDP) and its subsequent development as a leading anticancer drug.[2] These studies have not only broadened our understanding of the interactions of *cis*-DDP with the nitrogen bases of DNA,[3] its proposed biological target,[4] but have also provided insight into the chemistry of platinum in the unusual +3 oxidation state.[5] Another consequence of this work has been the complete structural characterization of one member of a long-known, but poorly understood, family of compounds referred to collectively as the platinum blues.[6] This compound, *cis*-diammineplatinum α-pyridone blue, has a zigzag chain of four Pt atoms with +2.25 average oxidation state.[6]

As described in reports appearing as early as 1908,[7] the oxidation of platinum(II) amide complexes produces intensely colored blue solutions from which paramagnetic blue-black powders have been isolated.[8] The spectroscopic properties of these powders, which exhibit one or more broad absorption bands in the 500–800-nm range,[8] are often similar to those of *cis*-diammineplatinum α-pyridone blue. Because the powders could not be crystallized for X-ray structural study, however, it has not been possible to make generalizations about their structures and the origin of their intense, low-energy optical transitions.

Recently several yellow tetranuclear Pt(II) complexes,[3b,9,10] a tetranuclear $Pt^{2.5}$ complex,[11] and two purported "nonstoichiometric" mixtures of $(Pt^{II})_4$, $(Pt^{2.25})_4$, and $(Pt^{2.5})_4$ species[12] have been structurally characterized. These geometric analogues of *cis*-diammineplatinum α-pyridone blue, however, do not exhibit the intense low-energy visible transitions typical of platinum blues.

In order to investigate the relationship between the stereochemistry of blue, mixed-valence Pt_4 chain complexes and their optical spectra, we undertook the synthesis of additional crystalline platinum blues. Specifically, we have isolated and structurally characterized a platinum α-pyridone blue with ethylenediamine as the equatorial, nonbridging ligand. Previous studies of its binuclear Pt(II) analogue revealed that steric interactions between adjacent ethylenediamine rings significantly alter the geometry[13]

(1) Rosenberg, B.; Van Camp, L. *Cancer Res.* **1970**, *30*, 1799.
(2) (a) Prestayko, A. E., Crooke, S. E., Carter, S. K., Eds. *Cisplatin, Status and New Developments*; Academic: New York, 1980. (b) Hacker, M. P., Douple, E. B., Krakoff, I. H., Eds. *Platinum Coordinaton Complexes in Cancer Chemotherapy*; Martinus Nijhoff: Boston, 1984.
(3) (a) For a review, see: Barton, J. K.; Lippard, S. J. In *Nucleic Acid–Metal Ion Interactions*; Spiro, T. G., Ed.; Wiley: New York, 1980; p 32. (b) Faggiani, R.; Lippert, B.; Lock, C. J. L. *Inorg. Chem.* **1980**, *19*, 295. (c) Faggiani, R.; Lock, C. J. L.; Pollock, R. J.; Rosenberg, B.; Turner, G. *Inorg. Chem.* **1981**, *20*, 804. (d) Lippert, B. *Inorg. Chem.* **1981**, *20*, 4326. (e) Lippert, B.; Neugebauer, D.; Raudaschl, G. *Inorg. Chim. Acta* **1983**, *105*, 161. (f) Hollis, L. S.; Lippard, S. J. *J. Am. Chem. Soc.* **1983**, *105*, 3494. (g) Fanchiang, Y.-T. *J. Chem. Soc., Dalton Trans* **1986**, 135 and references cited therein.
(4) Pinto, A.; Lippard, S. J. *Biochem. Biophys. Acta* **1985**, *780*, 167 and references cited therein.
(5) (a) O'Halloran, T. V.; Lippard, S. J. *Isr. J. Chem.* **1985**, *25*, 130. (b) Woollins, J. D.; Kelly, P. F. *Coord. Chem. Rev.* **1985**, *65*, 115.
(6) (a) Lippard, S. J. *Science (Washington, D.C.)* **1982**, *218*, 1075. (b) Barton, J. K.; Szalda, D. J.; Rabinowitz, H. N.; Waszczak, J. W.; Lippard, S. J. *J. Am. Chem. Soc.* **1979**, *101*, 1434. (c) Barton, J. K.; Caravana, C.: Lippard, S. J. *J. Am. Chem. Soc.* **1979**, *101*, 7269. (d) Barton, J. K.; Lippard, S. J. *Ann. N.Y. Acad. Sci.* **1978**, *313*, 686.
(7) Hoffmann, K. A.; Bugge, G. *Ber. Dtsch. Chem. Ges.* **1908**, *41*, 312.
(8) (a) Gillard, R. D.; Wilkinson, G. *J. Chem. Soc.* **1964**, 2835. (b) Davidson, J. P.; Faber, P. J.; Fischer, R. G., Jr.; Mansy, S.; Peresie, H. J.; Rosenberg, B.; Van Camp, L. *Cancer Chemother. Rep., Part 1* **1975**, *59*, 287. (c) Brown, D. B.; Burbank, R. D.; Robin, M. B. *J. Am. Chem. Soc.* **1969**, *91*, 2895. (d) Lerner, E. I. Ph.D. Dissertation, Columbia University, 1976. (e) Lippert, B. *J. Clin. Hematol. Oncol.* **1977**, *7*, 26. (f) Goodgame, D. M. L.; Jeeves, I. *Z. Naturforsch., C: Biosci.* **1979**, *34C*, 1287. (g) Woollins, J. D.; Rosenberg, B. *Inorg. Chem.* **1982**, *21*, 1280; *J. Inorg. Biochem.* **1983**, *19*, 41. (h) Appleton, T. G.; Berry, R. D.; Hall, J. R. *Inorg. Chim. Acta* **1982**, *64*, L229. (i) Seul, M.; Neubacher, H.; Lohmann, W. *Z. Naturforsch., B: Anorg. Chem., Org. Chem.* **1981**, *36B*, 651. (j) Laurent, J.-P.; Lepage, P. *Can. J. Chem.* **1981**, *59*, 1083. (k) Matsumoto, K.; Fuwa, K. *J. Am. Chem. Soc.* **1982**, *104*, 897. (l) Laurent, J.-P.; Lepage, P.; Castan, P.; Arrizabalaga, P. *Inorg. Chim. Acta* **1982**, *67*, 31. (m) Arrizabalaga, P.; Castan, P.; Laurent, J.-P. *J. Am. Chem. Soc.* **1984**, *106*, 4814. (n) Matsumoto, K.; Watanabe, T. *J. Am. Chem. Soc.* **1986**, *108*, 1308.
(9) Hollis, L. S.; Lippard, S. J. *J. Am. Chem. Soc.* **1981**, *103*, 1230; **1983**, *105*, 3494.
(10) Laurent, J.-P.; Lepage, P.; Dahan, F. *J. Am. Chem. Soc.* **1982**, *104*, 7335.
(11) (a) Matsumoto, K.; Takahashi, H.; Fuwa, K. *Inorg. Chem.* **1983**, *22*, 4086. (b) Matsumoto, K.; Fuwa, K. *J. Am. Chem. Soc.* **1982**, *104*, 897.
(12) (a) Matsumoto, K.; Takahashi, H.; Fuwa, K. *J. Am. Chem. Soc.* **1984**, *106*, 2049. (b) Matsumoto, K.; Fuwa, K. *Chem. Lett.* **1984**, 569. (c) Matsumoto, K. *Bull. Chem. Soc. Jpn.* **1985**, *58*, 651.

0020-1669/87/1326-1261$01.50/0

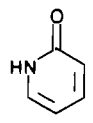
α-pyridone

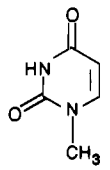
1-methyluracil (1-MeUH)

and reaction chemistry[14] of this complex in comparison to analogous complexes containing the *cis*-diammineplatinum moiety. We have also managed to crystallize *cis*-diammineplatinum 1-methyluracil blue, the existence of which has been previously established.[15] In this paper we describe the syntheses, crystal structures, magnetic properties, and visible spectra of these compounds, $[(en)Pt(C_5H_4NO)_2Pt(en)]_2(NO_3)_5\cdot H_2O$ (**1**) and $[(H_3N)_2Pt(C_5H_5N_2O_2)_2Pt(NH_3)_2]_2(NO_3)_5\cdot 5H_2O$ (**2**), and compare their properties to those of the *cis*-diammineplatinum α-pyridone analogue $[(H_3N)_2Pt(C_5H_4NO)_2Pt(NH_3)_2]_2(NO_3)_5\cdot H_2O$ (**3**). Moreover, we extend the previous SCF–Xα analysis[16] of **3** in a semiquantitative manner to correlate the Pt–Pt bond distances in these three compounds with the energies of their visible absorption bands and present a qualitative "particle-in-a-box" rationale linking the lowest energy intrachain charge-transfer band with the Pt_4 chain length. Aspects of this work have been communicated previously.[17]

Experimental Section

Preparation of Compounds. The starting materials HH-$[(en)Pt(C_5H_4NO)_2Pt(en)]_2(NO_3)_4$,[13] HH-$[(NO_3)(en)Pt(C_5H_4NO)_2Pt(en)(NO_2)](NO_3)_2\cdot 0.5H_2O$,[14b] *cis*-$[Pt(NH_3)_2(1\text{-}MeU)_2]\cdot 2H_2O$,[18] and *cis*-$[Pt(NH_3)_2I_2]$[19] were prepared as described in the literature. The first was recrystallized from water. Analytical data were obtained from Atlantic Microlab, Inc., Atlanta, GA.

(Ethylenediamine)platinum α-Pyridone Blue, $[(en)Pt(C_5H_4NO)_2Pt(en)]_2(NO_3)_5\cdot H_2O$ (1). This compound was obtained by first dissolving 70 mg (43 μmol) of the finely ground head-to-head Pt(II) complex $[(en)Pt(C_5N_4NO)_2Pt(en)]_2(NO_3)_2$ in 15 mL of H_2O at room temperature. Heating results in the head-to-head to head-to-tail isomerization described previously and should be avoided.[14a,c] A freshly prepared solution of 20 mg (21 μmol) of the binuclear Pt(III) complex HH-$[(NO_3)(en)Pt(C_5H_4NO)_2Pt(en)(NO_2)](NO_3)_2\cdot 0.5H_2O$ in 1 mL of 3 M HNO_3 was added to the solution. After the nitric acid concentration of the resulting mixture was adjusted to 0.5 M by adding ca. 0.5 mL of 16 M HNO_3, a blue-violet solution formed and was immediately frozen. The solution was placed in a freezer at 0 °C, following which blue-black needles mixed with a yellow-green powder formed. The crystals were manually removed and used in X-ray diffraction studies.

Alternatively, the deep blue-violet solutions could be frozen quickly in a dry ice–acetone bath. Warming to 4 °C and filtering gave ~40 mg (60%) of a blue powder. Yields typically ranged from 40 to 60%. The blue powder is only slightly soluble in dilute nitric acid solution but reasonably soluble in water. In the absence of nitric acid the blue-violet color rapidly fades, necessitating rapid recrystallization at low temperatures. The blue powder (40 mg) was stirred for ca. 30 s in 2 mL of H_2O at 4 °C. The solution was then filtered into a beaker containing ca. 0.1 mL of 16 M HNO_3 at 4 °C. The resulting blue-violet solution was stable at 4 °C, and after several hours at this temperature, the solution was filtered to yield 20 mg (50%) of blue-black microcrystals. Anal. Calcd for $Pt_4C_{28}H_{50}N_{17}O_{20}$ (**1**): C, 19.49; H, 2.92; N, 13.80. Found: C, 19.49, 19.39; H, 2.93, 2.88; N, 13.41, 13.39.

***cis*-Diammineplatinum 1-Methyluracil Blue, $[(H_3N)_2Pt(C_5H_5N_2O_2)_2Pt(NH_3)_2]_2(NO_3)_5\cdot 5H_2O$ (2).** A solution of 1 mmol of *cis*-$[Pt(NH_3)_2(H_2O)_2]^{2+}$ in 20–30 mL of water was prepared by mixing 500 mg of *cis*-$[Pt(NH_3)_2I_2]$ with 465 mg of $AgNO_3$ and filtering off the silver iodide. After 515 mg (1 mmol) of *cis*-$[Pt(NH_3)_2(1\text{-}MeU)_2]\cdot 2H_2O$ was added, the pH was adjusted to 5.5 and the solution was stirred at room temperature for 20 h. The initial yellow solution slowly turned purple during the course of the reaction. When 1 g of $NaNO_3$ and sufficient 7 M HNO_3 to adjust the pH to ~1 were added, the color changed to blue. After the mixture was cooled at 0 °C for 3 h, a crop of yellow-green crystals of the nitrate salt of the HH isomer of *cis*-$[(H_3N)_2Pt(C_5H_5N_2O_2)_2Pt(NH_3)_2]^{2+}$ were filtered off. To the resulting filtrate were added 3 g of solid $NaNO_3$ and 20 drops of 7 M HNO_3, and the temperature was raised to ~23 °C. A clear blue solution was obtained, cooled to 0 °C, and allowed to stand for 24 h, after which time the dark needles of *cis*-diammineplatinum 1-methyluracil blue that had deposited were filtered and dried. The yield was 30–35% of pure **2**, analytical data for which were reported previously.[17b] In 0.1 M HNO_3, compound **2** exhibits optical transitions at 740, 520, and 480 nm with molar extinction coefficients of ~9500, 900, and 900 M^{-1} cm^{-1}, respectively. The perchlorate salt was prepared in an analogous manner by substituting $HClO_4$ for HNO_3 and $NaClO_4$ for $NaNO_3$. The yield was 35%, and the product was identified by its optical [λ_{max} 740 (ϵ ~ 11 000 M^{-1} cm^{-1}) and 535 nm] and electron spin resonance spectra, which were similar to those of **2**.

Collection and Reduction of X-ray Data. $[(en)Pt(C_5H_4NO)_2Pt(en)]_2(NO_3)_5\cdot H_2O$ (1). A small black needle-like crystal (0.025 mm × 0.075 mm × 0.25 mm) was examined on the diffractometer by taking open-counter ω scans of several strong reflections. Its quality was judged to be acceptable for data collection ($\Delta\bar{\omega}_{1/2}$ ~ 0.4°).

The unit cell parameters (Table I) suggested that the crystal belongs to the triclinic system, but a systematic search using TRACER-II[20] revealed a possible cell of higher symmetry. Specifically, at DEL values of 1.0 or greater a *C*-centered monoclinic cell was found with a β angle of 127.72° and axis lengths a = 13.377 Å, b = 30.231 Å, and c = 9.413 Å. Zero- and first-level Weissenberg photographs, however, did not confirm the $2/m$ Laue symmetry expected for a monoclinic cell. In an additional test, the intensity data were transformed to the trial monoclinic system. Comparison of pairs of "equivalent" reflections always revealed very different intensities, further corroborating triclinic symmetry. The choice of space group $P\bar{1}$ (C_i^1)[21] was confirmed by the successful solution and refinement of the structure. Unit cell parameters and data collection procedures[22] are summarized in Table I.

$[(H_3N)_2Pt(C_5H_5N_2O_2)_2Pt(NH_3)_2]_2(NO_3)_5\cdot 5H_2O$ (2). A small dark blue needle having well-developed {100}, {010}, and {001} faces 0.1, 0.28, and 0.025 mm apart was mounted on a glass fiber for X-ray study. The crystal quality was marginally acceptable ($\Delta\bar{\omega}_{1/2}$ ~ 0.5° and diffraction only to 2θ ~ 40°), and the intensity standards deteriorated by 50% over time during data collection. The unit cell parameters, space group,[21] and data collection procedures[22] are given in Table I.

Structure Solution and Refinement. $[(en)Pt(C_5H_4NO)_2Pt(en)]_2(NO_3)_5\cdot H_2O$ (1). The structure was solved by the usual Patterson and Fourier methods and refined[23] with anisotropic thermal parameters for all non-hydrogen atoms. Anisotropic thermal parameters were also used in the refinement of a disordered nitrate (N6) and a partially occupied nitrate (N7) group. Refinement of the site occupation factor (SOF) for the latter nitrate gave 0.61, a value indicative of one-half nitrate per asymmetric unit. In general, refinement of the SOF is not in itself the best measure of occupancy, owing to correlation with thermal parameters. In this case, however, the thermal parameters are similar to those of the other nitrate groups. Moreover, the assignment of half-occupancy to nitrate (N7) is in agreement with the measured density, elemental analysis, and magnetic measurements.

Nitrate (N6) is partially disordered. While atoms O61, O62, and N6 were clearly observed, two peaks in the difference Fourier map appeared corresponding roughly to the position of the third oxygen, O63. This disorder was modeled as the superposition of two nitrate ions, where one nitrate group is formally related to the other by pivoting the entire group about the O61–O62 vector through a small angle θ. Upon refinement, the O61 and O62 positions did not change, N6 changed slightly, and O63 experienced the greatest amount of displacement in this formal rotation. Final refined site occupancy factors (SOF) of 0.54 (3) for O63A and 0.46

(13) Hollis, L. S.; Lippard, S. J. *Inorg. Chem.* **1983**, *22*, 2600.
(14) (a) O'Halloran, T. V.; Lippard, S. J. *J. Am. Chem. Soc.* **1983**, *106*, 3341. (b) O'Halloran, T. V.; Roberts, M. M.; Lippard, S. J. *Inorg. Chem.* **1986**, *25*, 957. (c) O'Halloran, T. V.; Lippard, S. J., to be submitted for publication.
(15) Lippert, B.; Neugebauer, D. *Inorg. Chem.* **1982**, *21*, 451.
(16) (a) Ginsberg, A. P.; O'Halloran, T. V.; Fanwick, P.; Hollis, L. S.; Lippard, S. J. *J. Am. Chem. Soc.* **1984**, *106*, 5430. (b) O'Halloran, T. V. Ph.D. Dissertation, Columbia University, 1985.
(17) (a) O'Halloran, T. V.; Roberts, M. M.; Lippard, S. J. *J. Am. Chem. Soc.* **1984**, *106*, 6427. (b) Mascharak, P. K.; Williams, I. D.; Lippard, S. J. *J. Am. Chem. Soc.* **1984**, *106*, 6428.
(18) Neugebauer, D.; Lippert, B. *J. Am. Chem. Soc.* **1982**, *104*, 6596.
(19) Dhara, S. G. *Indian J. Chem.* **1970**, *8*, 193.
(20) Lawton, S. L. "Tracer II, A FORTRAN Lattice Transformation–Cell Reduction Program"; Mobil Oil Corp.: Paulsboro, NJ, 1967.
(21) *International Tables for X-ray Crystallography*; Hahn, T., Ed., D. Reidel: Dordrecht: The Netherlands, 1983; Volume A, pp 104–105.
(22) Silverman, L. D.; Dewan, J. C.; Giandomenico, C. M.; Lippard, S. J. *Inorg. Chem.* **1980**, *19*, 3379.
(23) All calculations were performed on a DEC VAX 11/780 computer using SHELX-76: Sheldrick, G. M. In *Computing in Crystallography*; Schenk, H., Olthof-Hazekamp, R., van Konigsveld, H., Bassi, G. C., Eds.; Delft University Press: Delft, The Netherlands, 1978; pp 34–42.

Table I. Experimental Details of the X-ray Diffraction Studies for $[(en)Pt(C_5H_4NO)_2Pt(en)]_2(NO_3)_5\cdot H_2O$ (**1**) and $[(H_3N)_2Pt(C_5H_5N_2O_2)_2Pt(NH_3)_2]_2(NO_3)_5\cdot 5H_2O$ (**2**)

(A) Crystal Parameters[a]

	1	2		1	2
a, Å	10.652 (1)	10.123 (3)	space group	$P\bar{1}$	$P\bar{1}$
b, Å	13.068 (2)	13.084 (4)	Z	1	2
c, Å	9.413 (1)	19.508 (7)	V, Å^3	1157.7	2405.2
α, deg	108.14 (2)	92.28 (3)	ρ(calcd), g cm^{-3}	2.474	2.509 (2.430)[c]
β, deg	96.62 (1)	101.09 (3)	ρ(obsd), g cm^{-3}	2.485 (5)[b]	2.435 (13)[b]
γ, deg	68.39 (1)	107.49 (2)	M_r	1725.2	1817.1

(B) Measurement of Intensity Data[d]

	1	2
instrument	*g*	*g*
radiation	*h*	*h*
no. of reflcns collcd	4690 [$3° < 2\theta \leq 25°$ ($\pm h,\pm k,\pm l$); $25° < 2\theta < 50°$ ($h,\pm k,\pm l$)]	3691 ($3° < 2\theta < 40°$ ($h,\pm k,\pm l$)]

(C) Treatment of Intensity Data[d]

	1	2
μ, cm^{-1}	122.58	118.2
transmission factor range[e]	0.377–0.721	0.302–0.710
no. of unique reflcns after averaging	4009[f]	3015
no. of obsd unique data [$F_o > 4\sigma(F_o)$]	2918	2168

[a] From a least-squares fit of the setting angles of 25 reflections with $2\theta > 25°$. [b] By suspension in a mixture of $CHBr_3$ and $CHCl_3$ (four measurements) for **1** or by pycnometry for **2**. [c] The number in parentheses is for the sesquihydrate (see ref 17b, footnote 9). The density measurement was made on this material. [d] See ref 22 for typical procedures used in our laboratory. [e] Absorption corrections were performed with the Wehe–Busing–Levy ORABS program. [f] The agreement factor for averaging was 0.014. [g] Enraf-Nonius CAD-4F κ-geometry diffractometer. [h] Mo K$\bar{\alpha}$ (λ = 0.710 73 Å) graphite monochromatized.

(3) for O63B were consistent with this model of the nitrate ion disorder (vide supra).

Neutral-atom scattering factors and anomalous dispersion corrections for all non-hydrogen atoms were obtained from ref 24, and hydrogen atom scattering factors, from ref 25. The hydrogen atoms of α-pyridonate rings and of ethylenediamine carbon atoms were placed at calculated positions [d(C–H) = 0.95 Å] and constrained to "ride" on the carbon atoms to which they were attached.[23] The hydrogen atoms of the amine nitrogen atoms were also placed at calculated positions [d(N-H) = 0.95 Å] and refined as rigid groups. The hydrogen atoms of each α-pyridonate ring were given a common set of thermal parameters in the refinement. The hydrogen atoms of each carbon and nitrogen atom in the two ethylenediamine ligands also were given the same set of thermal parameters.

Full-matrix least-squares refinement of the structure using 293 parameters converged at $R_1 = 0.0305$ and $R_2 = 0.0387$. The function minimized during the refinement was $\sum w(|F_o| - |F_c|)^2$, where $w = 0.906/[\sigma^2(F_o) + 0.000625F_o^2]$. The maximum parameter shift in the final cycle of refinement was 1.09σ, associated with C1 (see below), and the only residual peaks of significance observed in the final difference Fourier map were within 0.9 Å of the platinum atoms (~1.7 e Å^{-3}). The average $w\Delta^2$ values for groups of data sectioned according to parity group, $(\sin\theta)/\lambda$, $|F_o|$, $|h|$, $|k|$, or $|l|$ showed good consistency, and the weighting function was found to be acceptable.

Final atomic positional parameters, together with their standard deviations, are reported in Table II. Interatomic distances and angles are given in Table IV. Tables S1 and S2 (supplementary material) contain, respectively, thermal parameters and observed and calculated structure factors for **1**.

$[(H_3N)_2Pt(C_5H_5N_2O_2)_2Pt(NH_3)_2]_2(NO_3)_5\cdot 5H_2O$ (2). Despite the falloff of intensity for the standard reflections during data collection, this structure was solved in a straightforward manner from Patterson and difference Fourier maps. Owing to the small data-to-parameter ratio, however, only the platinum atoms were refined anisotropically, while the other atoms were given isotropic thermal parameters. Of the five nitrate groups in the asymmetric unit, one was found to occupy two positions, disordered across crystallographic centers of symmetry, and refined with half-occupancy factors. Nitrate groups 3–6 were also refined with constraints such that N–O ~1.25 Å and O···O ~2.24 Å.[23] Hydrogen atoms of the 1-methyluracilate rings and the ammine ligands were constrained to idealized geometries[23] and given a common isotropic temperature factor, $U = 0.10$ Å^2. Hydrogen atoms on water molecules were not located. In the final refinement 323 parameters were varied, leading to $R_1 = 0.0388$ and $R_2 = 0.0429$. Weights were set as $w = 2.347[\sigma^2(F_o) + 0.000625F_o^2]$. The maximum parameter shift in the final refinement cycle was 2.6 σ, for nitrate group 3, and all other shifts were less than 0.1 σ. A final difference Fourier map had residual electron density near the water oxygen atoms of 1.0 e Å^{-3}, possibly due to hydrogens. Tables III and IV report final atomic positional parameters and interatomic distances and angles. Thermal parameters may be found in Table S3 (supplementary material) and observed and calculated structure factors, in Table S4 (supplementary material). Hydrogen atom parameters are reported in Table S5 (supplementary material).

Physical Measurements. Electron spin resonance spectra were recorded on a Varian E-line, X-band spectrometer operating at 3400 kG. Magnetic susceptibility measurements on 11.56 mg of **1** and 18.86 mg of **2** were carried out on a SHE Model 905 SQUID-type variable-field susceptometer operating at 20 kG. A total of 78 (for **1**) and 55 (for **2**) data points were taken over the range 7.0–302.1 K. At several temperatures the magnetic moment was measured as a function of field between 2 and 30 kG, revealing the presence of a small amount of ferromagnetic impurity. Extrapolating to infinite field (saturating conditions for ferromagnetism) revealed no field dependence for **2**. For **1**, the ferromagnetic contribution varied from 0.2% at 35 K to ca. 3.0% of the susceptibility at 290 K, so the susceptibility data were not corrected. Diamagnetic corrections of 633×10^{-6} cgsu for **1** and 622×10^{-6} cgsu for **2** were calculated from Pascal's constants.[26] Data were fit to a Curie–Weiss law by a nonlinear least squares method using a locally written program[27] on a VAX 11/780 computer.

Results and Discussion

Synthesis. Two synthetic routes were employed in the present study to obtain crystalline samples of platinum blues **1** and **2**. Addition of nitric acid (or perchloric acid to obtain the perchlorate salt) to oxidize the tetranuclear Pt(II) complex HH-$[(NH_3)_2Pt(C_5H_5N_2O_2)_2Pt(NH_3)_2]_2^{2+}$ to *cis*-diammineplatinum 1-methyluracil blue (**2**) parallels the original synthesis of *cis*-diammineplatinum α-pyridone blue (**3**) although the tetranuclear platinum(II) intermediate was not isolated or characterized at the time.[28] The preparation of **2** had been previously achieved by oxidation of the same HH-platinum(II) precursor with 0.1 M silver ion, pH 2–3.[15] The properties of **2** prepared by these two different methods appear to be identical. Compound **1** was ob-

(24) *International Tables for X-ray Crystallography*; Kynoch: Birmingham, England, 1974; Vol. IV, pp 99, 149.
(25) Stewart, R. F.; Davidson, E. R.; Simpson, W. T. *J. Chem. Phys.* **1965**, *42*, 3175.
(26) Earnshaw, A. *Introduction to Magnetochemistry*; Academic: New York; 1968.
(27) Karlin, K. D. Ph.D. Dissertation, Columbia University, 1975.
(28) (a) Barton, J. K.; Rabinowitz, H. N.; Szalda, D. J.; Lippard, S. J. *J. Am. Chem. Soc.* **1977**, *99*, 2827. (b) Barton, J. K.; Best, S. A.; Lippard, S. J.; Walton, R. A. *J. Am. Chem. Soc.* **1978**, *100*, 3785.

Table II. Final Positional Parameters for $[(en)Pt(C_5H_4NO)_2Pt(en)]_2(NO_3)_5 \cdot H_2O$ (1)[a,b]

ATOM	X	Y	Z
PT1	0.31138(4)	-0.29885(3)	-0.23942(4)
PT2	0.09253(4)	-0.11347(3)	-0.07648(4)
O12	0.0816(7)	-0.0641(6)	-0.2644(8)
O22	0.2470(6)	-0.0550(6)	0.0037(8)
N1	0.2171(9)	-0.3751(7)	-0.4227(9)
H1N1	0.2455(9)	-0.3700(7)	-0.5115(9)
H2N1	0.1221(9)	-0.3375(7)	-0.4123(9)
N21	0.4179(8)	-0.2322(7)	-0.0656(8)
N4	0.0883(8)	-0.1629(8)	0.1065(9)
H1N4	0.0759(8)	-0.0995(8)	0.1941(9)
H2N4	0.1710(8)	-0.2227(8)	0.1136(9)
N2	0.3329(10)	-0.4392(7)	-0.1739(9)
H1N2	0.2940(10)	-0.4147(7)	-0.0777(9)
H2N2	0.4262(10)	-0.4828(7)	-0.1698(9)
N11	0.3027(8)	-0.1740(7)	-0.3311(8)
N3	-0.0654(8)	-0.1668(7)	-0.1422(10)
H1N3	-0.0551(8)	-0.2089(7)	-0.2452(10)
H2N3	-0.1466(8)	-0.1017(7)	-0.1282(10)
C22	0.3702(10)	-0.1224(9)	0.0195(11)
C23	0.4541(11)	-0.0771(11)	0.1275(13)
H23	0.4194(11)	0.0011(11)	0.1860(13)
C25	0.6267(11)	-0.2604(11)	0.0679(12)
H25	0.7143(11)	-0.3104(11)	0.0845(12)
C26	0.5457(10)	-0.3004(10)	-0.0424(11)
H26	0.5782(10)	-0.3782(10)	-0.1027(11)
C24	0.5813(11)	-0.1458(11)	0.1507(12)
H24	0.6383(11)	-0.1149(11)	0.2224(12)
C16	0.4149(11)	-0.1918(10)	-0.4063(12)
H16	0.4959(11)	-0.2522(10)	-0.3960(12)
C12	0.1887(10)	-0.0881(8)	-0.3414(11)
C13	0.1846(11)	-0.0177(10)	-0.4309(11)
H13	0.1036(11)	0.0436(10)	-0.4381(11)
C14	0.2962(13)	-0.0394(10)	-0.5079(13)
H14	0.2926(13)	0.0045(10)	-0.5730(13)
C15	0.4166(13)	-0.1252(12)	-0.4905(13)
H15	0.4970(13)	-0.1377(12)	-0.5384(13)
C1	0.243(2)	-0.4924(13)	-0.4288(17)
H1C1	0.327(2)	-0.5350(13)	-0.4786(17)
H2C1	0.176(2)	-0.5198(13)	-0.4840(17)
C2	0.2664(15)	-0.5145(11)	-0.2852(15)
H2C2	0.1787(15)	-0.4958(11)	-0.2490(15)
H1C2	0.3176(15)	-0.5929(11)	-0.2939(15)
C3	-0.0751(17)	-0.2362(15)	-0.054(2)
H1C3	-0.0207(17)	-0.3134(15)	-0.102(2)
H2C3	-0.1662(17)	-0.2310(15)	-0.052(2)
C4	-0.0236(17)	-0.2086(14)	0.0889(16)
H1C4	-0.0971(17)	-0.1491(14)	0.1472(16)
H2C4	0.0048(17)	-0.2735(14)	0.1258(16)
N5	0.3311(12)	-0.3611(10)	0.2633(10)
O51	0.4032(9)	-0.4337(8)	0.3264(9)
O52	0.2227(10)	-0.2855(8)	0.3245(10)
O53	0.3661(11)	-0.3625(12)	0.1405(10)
N6	0.8342(16)	-0.2457(14)	0.5049(19)
O61	0.8068(15)	-0.2515(14)	0.3721(20)
O62	0.7449(15)	-0.2176(14)	0.5927(18)
O63A[c]	0.9446(19)	-0.2338(18)	0.5272(20)
O63B[c]	0.940(2)	-0.3117(20)	0.561(2)
N7[d]	0.0712(17)	-0.497(2)	0.1098(19)
O71[d]	0.0977(16)	-0.5015(16)	0.2390(15)
O72[d]	0.1485(17)	-0.4787(20)	0.0408(19)
O73[d]	-0.0471(15)	-0.478(2)	0.0642(19)

[a] Numbers in parentheses are errors in the last significant digit(s). [b] The atom labeling scheme is given in Figure 1. [c] Disordered oxygen atoms with occupancy factors of 0.54 (3) for O63A and 0.46 (3) for O63B. [d] Refined as a rigid group with an occupancy factor of 0.5.

tained by an alternative, electron-transfer route, in which a 2:1 ratio of HH-$[(en)Pt(C_5H_4NO)_2Pt(en)]_2(NO_3)_4$ and HH-$[(O_2N)(en)Pt(C_5H_4NO)_2Pt(en)(NO_3)](NO_3)_2 \cdot 0.5H_2O$ was allowed to react. Because of the propensity of the former to isomerize,[14a] heating must be avoided in this reaction. The binuclear head-to-tail (HT) isomers cannot, for stereochemical reasons,[6a] aggregate and be oxidized to form mixed-valent tetranuclear platinum blues.

Description of the Structures. (Ethylenediamine)platinum α-Pyridone Blue (1). As shown in Figure 1, the tetranuclear cation is composed of two binuclear, α-pyridonate-bridged moieties related through a crystallographic inversion center that lies at the midpoint of the Pt2–Pt2′ vector. The distance between the α-pyridonate-bridged platinum atoms Pt1 and Pt2 of 2.8296 (5) Å is 0.0762 (7) Å shorter than the inner Pt2–Pt2′ distance of 2.9158

Table III. Final Non-Hydrogen Atom Positional Parameters for $[(H_3N)_2Pt(C_5H_5N_2O_2)_2Pt(NH_3)_2]_2(NO_3)_5 \cdot 5H_2O$ (2)[a,b]

ATOM	X	Y	Z
Pt1	0.98461(11)	0.59867(8)	0.77722(5)
Pt2	0.93518(11)	0.37511(8)	0.76070(5)
Pt3	0.96353(12)	1.16412(8)	0.74827(5)
Pt4	0.91471(11)	0.94329(8)	0.72027(5)
N11	1.134(2)	0.5902(15)	0.8604(9)
C12	1.174(3)	0.5024(20)	0.8785(12)
O13	1.1056(17)	0.4131(12)	0.8405(8)
C14	1.284(3)	0.5084(19)	0.9364(12)
C15	1.343(3)	0.6042(19)	0.9762(12)
N16	1.309(2)	0.6905(15)	0.9625(10)
C17	1.377(3)	0.792(2)	1.0052(15)
C18	1.203(3)	0.691(2)	0.9051(13)
O19	1.1644(19)	0.7690(15)	0.8900(9)
N21	1.1185(20)	0.6000(15)	0.7122(9)
C22	1.134(3)	0.5110(20)	0.6851(12)
O23	1.0643(17)	0.4163(13)	0.6923(8)
C24	1.236(3)	0.519(2)	0.6376(13)
C25	1.305(3)	0.620(2)	0.6248(14)
N26	1.289(2)	0.7111(16)	0.6551(10)
C27	1.362(3)	0.816(2)	0.6376(14)
C28	1.189(3)	0.703(2)	0.6970(13)
O29	1.1769(18)	0.7834(14)	0.7264(9)
N1	0.848(2)	0.6111(15)	0.8417(10)
N2	0.842(2)	0.6170(15)	0.6953(10)
N3	0.811(2)	0.3229(15)	0.8296(10)
N4	0.764(2)	0.3286(15)	0.6807(10)
N5	1.146(2)	0.2272(16)	0.7127(10)
N6	1.077(2)	0.1913(16)	0.8492(10)
N7	1.064(2)	-0.0559(16)	0.6635(11)
N8	1.042(2)	-0.0871(15)	0.8074(10)
N31	0.789(2)	-0.0372(14)	0.6309(9)
C32	0.787(3)	0.0612(18)	0.6075(12)
O33	0.8578(17)	0.1474(12)	0.6472(8)
C34	0.720(2)	0.0629(18)	0.5407(12)
C35	0.653(3)	-0.0325(20)	0.4981(13)
N36	0.651(2)	-0.1245(15)	0.5213(10)
C37	0.574(3)	-0.224(2)	0.4734(14)
C38	0.714(3)	-0.1287(19)	0.5844(12)
O39	0.7182(19)	-0.2148(15)	0.6102(9)
N41	0.751(2)	-0.0706(17)	0.7728(10)
C42	0.716(3)	0.013(2)	0.7913(12)
O43	0.7801(16)	0.1100(12)	0.7830(7)
C44	0.592(3)	-0.005(2)	0.8198(13)
C45	0.520(3)	-0.110(2)	0.8294(13)
N46	0.566(2)	-0.1908(15)	0.8114(10)
C47	0.494(3)	-0.301(2)	0.8219(13)
C48	0.680(3)	-0.171(2)	0.7826(13)
O49	0.7268(19)	-0.2442(15)	0.7662(9)
NO1	0.456(3)	0.133(2)	0.7050(14)
O1A	0.506(2)	0.2038(16)	0.7549(11)
O1B	0.531(2)	0.1101(16)	0.6697(11)
O1C	0.330(3)	0.089(2)	0.6922(14)
NO2	0.457(3)	0.3925(19)	0.8299(13)
O2A	0.396(2)	0.3236(15)	0.8655(10)
O2B	0.389(2)	0.4170(14)	0.7778(10)
O2C	0.590(2)	0.4293(16)	0.8482(11)
NO3	0.212(4)	0.154(2)	0.031(2)
O3A	0.135(4)	0.142(3)	0.0775(17)
O3B	0.275(5)	0.250(3)	0.020(3)
O3C	0.245(4)	0.076(3)	0.0063(20)
NO4	0.057(5)	0.193(2)	0.5188(14)
O4A	0.094(3)	0.2767(18)	0.5630(13)
O4B	0.068(3)	0.1057(17)	0.5432(13)
O4C	0.009(3)	0.212(2)	0.4573(13)
NO5	0.5000	0.5000	0.5000
O5A	0.534(5)	0.508(3)	0.4419(12)
O5B	0.591(5)	0.493(4)	0.5528(18)
O5C	0.623(3)	0.504(7)	0.495(3)
NO6	1.0000	0.5000	1.0000
O6A	0.959(6)	0.576(3)	0.979(3)
O6B	0.956(6)	0.4037(17)	0.975(3)
O6C	0.907(2)	0.477(2)	0.9470(9)
OW1	0.567(2)	0.4525(14)	0.6822(9)
OW2	0.833(3)	0.3475(18)	0.5414(12)
OW3	0.691(3)	-0.0811(19)	1.1345(12)
OW4	0.891(4)	0.582(3)	0.5496(18)
OW5	0.891(4)	0.126(3)	0.9476(20)

[a] See footnote *a*, Table II. [b] Atoms are labeled as shown in Figure 2. [c] Nitrate groups 5 and 6 are disordered on crystallographic centers of symmetry and are assigned half-occupancy.

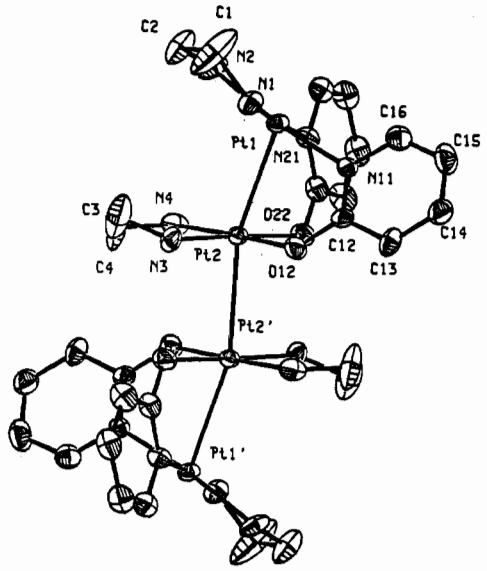

Figure 1. Structure of the cation in **1** showing the 40% probability thermal ellipsoids and atom-labeling scheme. Primed and unprimed atoms are related by a crystallographically required center of symmetry.

Å. The angle between the Pt1–Pt2 and Pt2–Pt2′ vectors in the four-atom, zigzag chain is 164.33 (3)°. Bond distances and angles (Table IV) within the platinum coordination planes compare favorably with values found in related amidate-bridged or ethylenediamine complexes[13,29] of platinum in the +2 or +2.25 average oxidation state.[6,12] As with several other α-pyridonate-bridged platinum complexes, the Pt–N(amine) distances trans to the pyridonate nitrogen atoms are slightly longer (ca. 2σ) than those trans to the pyridonate oxygen atoms, revealing a small trans influence. A recent SCF–Xα calculation on *cis*-diammineplatinum α-pyridone blue (**3**) revealed that, in this case, the trans influence originates in more extensive σ-overlap of the Pt–N(heterocycle) bond relative to the Pt–O(amidate) bond.[16]

Both platinum coordination spheres are planar with four-atom root-mean-square deviations of 0.259 Å for the Pt1 plane and 0.014 Å for the Pt2 plane. As observed in all α-pyridonate-bridged platinum complexes regardless of the oxidation state, the platinum atoms are slightly displaced out of the ligand planes toward one another, by 0.097 Å for Pt1 and 0.0287 Å for Pt2. The average torsion angle, ω, about the Pt1–Pt2 vector is 24.3° and the tilt (τ) between the Pt1 and Pt2 coordination planes is 32.1°.

Comparison of the bond lengths and angles within the two α-pyridonate rings shows that both rings have equivalent geometries. The bite distances in the two amidate rings are similar (O12–N11 = 2.30 (1) Å, O22–N21 = 2.31 (1) Å), and both geometries reveal the usual changes accompanying platinum coordination.[9,30]

Hydrogen bonds connecting the two binuclear subunits across the inversion center occur between N3 and O22′. The tetranuclear units are further linked through a network of hydrogen bonds between the amine ligands and nitrate anions. The bond lengths and angles of the N5 and N7 nitrate anions are normal, and both are planar within ±0.05 Å. Oxygen atom O51 of the N5-nitrate anion is 3.60 Å from Pt1 at the end of the tetranuclear Pt_4 chain. In **3** the corresponding distance was 3.32 Å.[6b]

Both forms of the disordered nitrate N6 are approximately planar. The four-atom root-mean-square deviations were 0.063 Å (N6–O61–O62–O63A) and 0.088 Å (N6–O61–O62–O63B). The N6 atoms were displaced from the plane by 0.11 and 0.15 Å, respectively. The nitrate oxygen bond lengths were normal, as is the O61–N6–O62 angle. However, the angles O61–N6–O63A and O62–N6–O63B showed significant deviations from the typical range of 115–124°. These deviations, as well as the large thermal parameters of N6, result in part from attempts to model the electron density by static disorder as described above. The crystal structure of the nearly isomorphous *cis*-diammineplatinum σ-pyridone blue (**3**) also revealed a partially disordered nitrate anion in the same region of the unit cell.[6b]

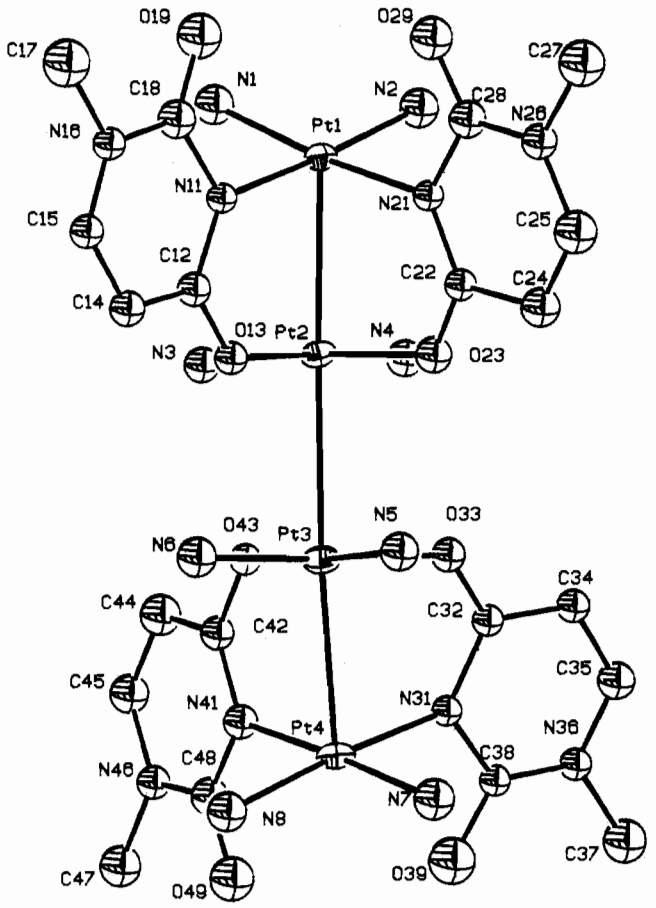

Figure 2. Structure and atom labels of the cation in **2**.

Elemental analysis and density measurements indicate the presence of a water of hydration. No crystallographic evidence was found, however, for this water molecule. In the nearly isomorphous *cis*-diammineplatinum complex **3**, a disordered water molecule was located close to the nitrate ion that was disordered across an inversion center.[6b] The proximity of a water molecule to the disordered nitrate group in **1** and the possible loss of water of hydration during data collection (the crystal was not enclosed in a capillary, and the intensity standards fell by 15% during data collection) could well account for the failure to define its position crystallographically.

An extensive series of inter- and intracation hydrogen bonds occur in the crystal structure (Table IV). The tetranuclear cation is stabilized by hydrogen bonding between ligands coordinated to Pt2 and Pt2′, specifically between protons on the ethylenediamine nitrogen atoms and the α-pyridonate oxygen atoms. Similar hydrogen bonding occurs in **3**.[6b] Bond lengths and angles within the ethylenediamine rings are normal[29] and reflect high thermal motion or possible slight disorder of the methylene carbon atoms (see Figure 1). The N1–C1–C2–N2 and N3–C3–C4–N4 torsion angles are −37.0 and −35.4°, respectively.

***cis*-Diammineplatinum 1-Methyluracil Blue (2).** Figure 2 displays the structure of the tetranuclear cation in **2**. In this platinum blue the halves of the cation are crystallographically independent, which allows the coordination planes of the inner pair of platinum atoms to twist (ω value 22.3°) with respect to each other, rather than be eclipsed (ω = 0°), as is the case for **1** and **3**. On the other hand, the twist angles about the outer two metal–metal bonds are 6.12° for Pt1–Pt2 and 8.53° for Pt3–Pt4.

(29) (a) Faggiani, R.; Lippert, B.; Lock, C. J. L. *Inorg. Chem.* **1980**, *19*, 295. (b) Gellert, R. W.; Bau, R. *J. Am. Chem. Soc.* **1975**, *97*, 7380. (c) Neidle, S.; Taylor, G. L.; Robbins, A. B. *Acta Crystallogr., Sect. B: Struct. Crystallogr. Cryst. Chem.* **1978**, *B34*, 1838.
(30) Hollis, L. S.; Lippard, S. J. *Inorg. Chem.* **1983**, *22*, 2605.

Table IV. Selected Interatomic Distances (Å) and Angles (deg) for $[(en)Pt(C_5H_4NO)_2Pt(en)]_2(NO_3)_5 \cdot H_2O$ (**1**) and $[(H_3N)_2Pt(C_5H_5N_2O_2)_2Pt(NH_3)_2]_2(NO_3)_5 \cdot 5H_2O$ (**2**)[a]

Coordination Spheres					
1		**2**			
Pt1–Pt2	2.8296 (5)	Pt1–Pt2	2.810 (2)	Pt2–Pt3	2.866 (2)
		Pt3–Pt4	2.793 (2)		
Pt1–N1	2.060 (9)	Pt1–N1	2.07 (2)	Pt1–N2	2.01 (2)
Pt1–N2	2.040 (10)	Pt1–N11	2.03 (2)	Pt1–N21	2.02 (2)
Pt1–N21	2.034 (8)	Pt2–O13	2.01 (1)	Pt2–N3	2.02 (2)
Pt2–Pt2′	2.9158 (6)	Pt2–N4	2.01 (2)	Pt2–O23	2.02 (2)
Pt2–N3	2.014 (10)	Pt3–O33	2.02 (1)	Pt3–O43	2.04 (2)
Pt2–N4	2.029 (10)	Pt3–N5	2.04 (2)	Pt3–N6	2.04 (2)
Pt2–O22	2.036 (8)	Pt4–N7	2.04 (2)	Pt4–N8	2.05 (2
		Pt4–N31	2.03 (2)	Pt4–N41	2.08 (2)
Pt1–Pt2–Pt2′	164.33 (3)	N2–Pt1–N21	89.2 (8)	N2–Pt1–N11	176.4 (7)
N1–Pt1–N2	83.8 (4)	N2–Pt1–N1	88.4 (9)	N2–Pt1–Pt2	101.5 (5)
N1–Pt1–N11	91.7 (4)	N21–Pt1–N11	90.4 (8)	N21–Pt1–N1	174.9 (8)
N1–Pt1–N21	175.7 (3)	N21–Pt1–Pt2	83.1 (5)	N11–Pt1–N1	91.8 (8)
N2–Pt1–N11	172.2 (3)	N11–Pt1–Pt2	82.0 (5)	N1–Pt1–Pt2	101.8 (5)
N2–Pt1–N21	95.3 (4)	O13–Pt2–N4	176.9 (8)	O13–Pt2–N3	89.0 (7)
N11–Pt1–N21	88.8 (4)	O13–Pt2–O23	89.8 (6)	O13–Pt2–Pt1	82.0 (5)
N3–Pt2–N4	83.7 (4)	O13–Pt2–Pt3	87.0 (5)	N4–Pt2–N3	90.4 (8)
N3–Pt2–O12	91.9 (4)	N4–Pt2–O23	90.5 (7)	N4–Pt2–Pt1	101.1 (6)
N3–Pt2–O22	176.2 (3)	N4–Pt2–Pt3	89.9 (6)	N3–Pt2–O23	175.3 (8)
N4–Pt2–O12	175.4 (3)	N3–Pt2–Pt1	102.0 (6)	N3–Pt2–Pt3	87.8 (6)
N4–Pt2–O22	93.5 (4)	O23–Pt2–Pt1	82.2 (5)	O23–Pt2–Pt3	87.6 (5)
O12–Pt2–O22	90.8 (3)	Pt1–Pt2–Pt3	165.02 (5)		
		O33–Pt3–O43	92.2 (6)	O33–Pt3–N6	176.2 (7)
		O33–Pt3–N5	87.0 (7)	O33–Pt3–Pt4	82.4 (5)
		O33–Pt3–Pt2	87.5 (5)	O43–Pt3–N6	90.2 (7)
		O43–Pt3–N5	176.5 (8)	O43–Pt3–Pt4	81.8 (5)
		O43–Pt3–Pt2	87.3 (5)	N6–Pt3–N5	90.5 (8)
		N6–Pt3–Pt4	100.9 (6)	N6–Pt3–Pt2	89.6 (6)
		N5–Pt3–Pt4	101.4 (6)	N5–Pt3–Pt2	89.4 (6)
		Pt4–Pt3–Pt2	164.81 (5)		
		N31–Pt4–N7	88.1 (8)	N31–Pt4–N8	175.8 (8)
		N31–Pt4–N41	89.9 (8)	N31–Pt4–Pt3	82.7 (5)
		N7–Pt4–N8	90.1 (9)	N7–Pt4–N41	174.8 (7)
		N7–Pt4–Pt3	100.8 (6)	N8–Pt4–N41	91.6 (8)
		N8–Pt4–Pt3	101.3 (5)	N41–Pt4–Pt3	83.6 (6)
Ligand Geometry for **1**					
Ethylenediamine Ligands					
N1–C1	1.44 (2)	C2–N2	1.51 (2)	C3–C4	1.39 (2)
C1–C2	1.44 (2)	N3–C3	1.44 (3)	C4–N4	1.49 (2)
Pt1–N1–C1	110.2 (8)	N1–C1–C2	114.6 (11)	Pt2–N4–C4	108.7 (8)
Pt1–N2–C2	110.2 (8)	Pt2–N3–C3	111.0 (9)	N3–C3–C4	113.2 (17)
α-Pyridonate Ligands					
O12–C12	1.31 (1)	C15–C16	1.35 (2)	C23–C24	1.36 (1)
N11–C12	1.33 (1)	C16–N11	1.37 (2)	C24–C25	1.38 (2)
C12–C13	1.41 (2)	O22–C22	1.31 (1)	C25–C26	1.37 (2)
C13–C14	1.36 (2)	N21–C22	1.34 (1)	C26–N21	1.36 (1)
C14–C15	1.39 (1)	C22–C23	1.41 (2)		
Pt1–N11–C12	123.2 (10)	O12–C12–N11	121.0 (11)	O22–C22–N21	121.4 (9)
Pt1–N11–C16	116.7 (7)	O12–C12–C13	119.0 (8)	O22–C22–C23	118.6 (9)
Pt2–O12–C12	122.3 (6)	N11–C12–C13	119.9 (10)	N21–C22–C23	120.0 (8)
Pt1–N21–C22	122.4 (6)	C12–C13–C14	119.7 (10)	C22–C23–C24	120.2 (10)
Pt1–N21–C26	118.0 (6)	C13–C14–C15	120.0 (13)	C23–C24–C25	119.2 (10)
Pt2–O22–C22	123.3 (7)	C15–C16–N11	122.9 (10)	C25–C26–N21	121.7 (9)
C12–N11–C16	119.2 (10)	C22–N21–C26	119.4 (8)		
Ligand Geometry for **2**					
1-Methyluracilate Ligands					
N11–C12	1.37 (4)	N11–C18	1.46 (3)	N31–C32	1.39 (3)
C12–O13	1.28 (3)	C12–C14	1.40 (3)	C32–O33	1.27 (2)
C14–C15	1.35 (3)	C15–N16	1.30 (4)	C34–C35	1.38 (3)
N16–C18	1.39 (3)	N16–C17	1.44 (3)	N36–C38	1.29 (3)
C18–O19	1.22 (4)			C38–O39	1.26 (3)
N21–C22	1.32 (3)	N21–C28	1.40 (3)	N41–C42	1.31 (4)
C22–O23	1.26 (3)	C22–C24	1.50 (4)	C42–O43	1.27 (3)
C24–C25	1.35 (4)	C25–N26	1.38 (4)	C44–C45	1.40 (3)
N26–C28	1.40 (4)	N26–C27	1.44 (3)	N46–C48	1.34 (4)
C28–O29	1.22 (4)			C48–O49	1.25 (4)
C42–N41–C48	122 (2)	N46–C45–C44	120 (3)	C42–N41–Pt4	122 (2)

N31–C38	1.39 (3)		
C32–C34	1.35 (3)		
C35–N36	1.30 (3)		
N36–C37	1.48 (3)		
N41–C48	1.34 (3)		
C42–C44	1.43 (4)		
C45–N46	1.33 (4)		
N46–C47	1.45 (3)		
C45–N46–C48	120 (2)		

Table IV (Continued)

C48–N41–Pt4	116 (2)	C45–N46–C47	121 (2)	O43–C42–N41	125 (3)	C48–N46–C47	119 (2)
O43–C42–C44	117 (3)	O49–C48–N41	117 (3)	N41–C42–C44	118 (2)	O49–C48–N46	122 (2)
C42–O43–Pt3	127 (2)	N41–C48–N46	121 (3)	C45–C44–C42	118 (3)		

Anion Geometry

1		2			
N5–O51	1.25 (1)	NO1–O1A	1.23 (3)	NO1–O1B	1.22 (4)
N5–O52	1.26 (1)	NO1–O1C	1.20 (4)	NO2–O2A	1.25 (3)
N5–O53	1.25 (2)	NO2–O2B	1.23 (3)	NO2–O2C	1.26 (3)
N6–O61	1.24 (2)	NO3–O3A	1.28 (6)	NO3–O3B	1.28 (5)
N6–O62	1.21 (2)	NO3–O3C	1.27 (6)	NO4–O4A	1.28 (3)
N6–O63A	1.23 (3)	NO4–O4B	1.28 (4)	NO4–O4C	1.27 (4)
N6–O63B	1.31 (3)	NO5–O5A	1.25 (4)	NO5–O5B	1.27 (4)
N7–O71	1.23 (2)	NO5–O5C	1.25 (4)	NO6–O6A	1.23 (4)
N7–O72	1.23 (4)	NO6–O6B	1.25 (4)	NO6–O6C	1.21 (4)
N7–O73	1.24 (2)				
O51–N5–O52	119.7 (11)	O1C–NO1–O1B	121 (3)	O1C–NO1–O1A	118 (3)
O51–N5–O53	120.1 (10)	O1B–NO1–O1A	121 (3)	O2B–NO2–O2A	120 (2)
O52–N5–O53	120.1 (11)	O2B–NO2–O2C	123 (2)	O2A–NO2–O2C	117 (2)
O61–N6–O62	119.9 (17)	O3C–NO3–O3B	119 (5)	O3C–NO3–O3A	122 (3)
O61–N6–O63A	106.2 (20)	O3B–NO3–O3A	118 (4)	O4C–NO4–O4A	112 (3)
O61–N6–O63B	128.2 (15)	O4C–NO4–O4B	131 (3)	O4A–NO4–O4B	117 (3)
O62–N6–O63A	129.1 (17)	O5A–NO5–O5B′	118 (3)	O5A–NO5–O5C′	120 (3)
O62–N6–O63B	104.1 (19)	O5B′–NO5–O5C′	121 (3)	O6A–NO6–O6B′	128 (2)
O71–N7–O72	120.1 (19)	O6A–NO6–O6C′	130 (3)	O6B′–NO6–O6C′	127 (3)
O71–N7–O73	119.4 (20)				
O72–N7–O73	117.4 (23)				

Hydrogen Bonds

1		2			
H2N3–O22′	1.97 (1)	N5–O23	2.85 (3)	N2–OW4	3.02 (4)
H1N4–O12′	2.13 (1)	N6–O13	2.84 (3)	N4–OW2	2.93 (3)
H1N1–O52′	2.11 (2)	N4–O33	2.90 (3)	N6–OW5	2.92 (5)
H1N1–O51′	2.15 (1)	N3–O43	2.80 (3)	N2–OW1	2.92 (3)
H2N1–O63B′	1.85 (2)	N4–OW1	2.93 (3)	N6–OW3	3.08 (4)
H2N1–O63A′	2.02 (2)	N8–OW3	2.92 (3)	O2B–OW1	2.79 (3)
H1N2–O53	2.10 (1)	O3C–OW5	2.86 (5)	O4A–OW4	2.92 (4)
H2N2–O51′	2.20 (1)	O5B–OW4	2.92 (6)	O5C–OW4	2.59 (5)
H1N3–O63B′	1.91 (2)	OW2–OW4	2.94 (4)	O4A–OW2	3.01 (4)
H1N3–O63A′	2.06 (2)	O2A–OW3	3.03 (3)	O4C–OW4	2.60 (4)
H2N4–O53	2.26 (1)	O2C–OW1	3.23 (3)	O5A–OW1	2.58 (3)
H2N4–O52	2.31 (1)	O3A–OW5	3.13 (5)	O5B–OW1	2.64 (4)
		O3C–OW3	2.94 (5)		
N3–H2N3–O22′	147.0 (9)				
N4–H1N4–O12′	132.6 (8)				
O52–H1N1–N1	151.4 (8)				
O51–H1N1–N1	146.7 (9)				
O63B–H2N1–N1	160.2 (11)				
O63A–H2N1–N1	150.9 (13)				
O53–H1N2–N2	133.2 (11)				
O51–H2N2–N2	136.2 (9)				
O63B–H1N3–N3	165.8 (15)				
O63A–H1N3–N3	156.9 (12)				
O53–H2N4–N4	177.7 (9)				
O53–H2N4–N4	120.1 (9)				

[a] See footnotes to Tables II and III. Values are uncorrected for thermal motion.

The outer pairs of Pt–Pt bonds [2.810 (1) and 2.793 (1) Å] are significantly shorter than the inner one [2.865 (1) Å], and angles of 165.0 (1) and 164.8 (1)° between adjacent pairs of Pt–Pt vectors characterize the zigzag tetraplatinum chain. Although errors in the individual bond lengths and angles within the platinum coordination planes and 1-methyluracil ligands (Table IV) are larger than usual, owing to the marginal quality of the crystals, comparisons with literature values in related 1-methyluracilate-bridged polynuclear platinum compounds show satisfactory (±3 esd) agreement.[3e,18,31]

Best planes calculations revealed no coordinated atom to deviate by more than 0.03 Å from its individual platinum coordination plane. Platinum atoms were displaced by amounts ranging from 0.03 to 0.06 Å in such a manner that atom pairs Pt1/Pt2 and Pt3/Pt4 move toward each other, as in **1** and **3**. Tilt angles (τ) between coordination planes are 27.3° for Pt1 and Pt2, 0.05° for Pt2 and Pt3, and 26.4° for Pt3 and Pt4. Thus, although the central two coordination planes are not required by symmetry to be parallel, as was the case in **1** and **3**, they are nearly so. In most respects, *cis*-diammineplatinum 1-methyluracil blue is structurally similar to its α-pyridone analogues.

Other features of the geometry, including possible hydrogen-bonding interactions in the crystal lattice, may be found in Table IV.

Structural Comparisons among Amidate-Bridged Tetranuclear Platinum Complexes. Table V lists structural features of the three crystalline platinum blues **1**–**3**, as well as several related tetranuclear analogues, excluding nonstoichiometric species.[12] The steric requirements of the nonbridging ligands introduce subtle

(31) Thewalt, U.; Neugebauer, D.; Lippert, B. *Inorg. Chem.* **1984**, *23*, 1713.

Table V. Comparison of Geometric Features of Amidate-Bridged Tetranuclear Platinum Complexes

compound	formal Pt oxidn state	Pt–Pt dist, Å	τ,[a] deg	ω,[b] deg	Pt–Pt–Pt angle, deg	ref
$[(en)Pt(C_5H_4NO)_2Pt(en)]_2(NO_3)_5\cdot H_2O$ (**1**)	2.25	2.8296 (5)[c] 2.9158 (5)	32.1	24.3	164.33 (3)	*d*
cis-$[(H_3N)_2Pt(C_5H_5N_2O_2)_2Pt(NH_3)_2]_2(NO_3)_5\cdot 5H_2O$ (**2**)	2.25	2.810 (2)[c] 2.866 (2) 2.793 (2)[c]	27.3 0.05[e] 26.4	6.1 22.1[e] 8.4	165.02 (5) 164.81 (5)	*d*
cis-$[(H_3N)_2Pt(C_5H_4NO)_2Pt(NH_3)_2]_2(NO_3)_5\cdot H_2O$ (**3**)	2.25	2.7745 (4)[c] 2.8770 (9)	27.4	22.8	164.20 (2)	6b
$[(en)Pt(C_5H_4NO)_2Pt(en)]_2(NO_3)_4$	2.0	2.992 (1)[c] 3.236 (1)	39.6	24.9	160.58 (3)	13
cis-$[(H_3N)_2Pt(C_5H_4NO)_2Pt(NH_3)_2]_2(NO_3)_4$	2.0	2.8767 (7)[c] 3.1294 (9)	30.0	20.3	158.40 (3)	9
cis-$[(H_3N)_2Pt(C_4H_6NO)_2Pt(NH_3)_2]_2(NO_3)_6\cdot 3H_2O$	2.5	2.702 (6)[c] 2.710 (5) 2.706 (6)[c]	18.7 21.2	4.3 5.1	170.4 (1)	11

[a] τ is the tilt angle between adjacent platinum coordination planes in the bridged binuclear units. [b] ω is the average torsion angle about the Pt–Pt vector in the bridged binuclear units. [c] Bridged Pt–Pt distance. [d] This work. [e] Value for unbridged Pt–Pt unit.

Table VI. Observed and Free Electron Model Calculated Visible Electronic Spectral Bands of the Platinum Blues

complex	Pt–Pt chain length,[a] Å	ΔE[b] obsd nm	obsd eV	calcd[c] nm	calcd eV
$[(en)Pt(C_5H_4NO)_2Pt(en)]_2^{5+}$ (**1**)	11.43	745	1.66	614	2.02
		532	2.33	287	4.32
				(359)	(3.45)
cis-$[(H_3N)_2Pt(C_5H_5N_2O_2)_2Pt(NH_3)_2]_2^{5+}$ (**2**)	11.29	740	1.67	602	2.06
		520	2.39	281	4.42
		480	2.58	(350)	(3.54)
cis-$[(H_3N)_2Pt(C_5H_4NO)_2Pt(NH_3)_2]_2^{5+}$ (**3**)	11.22	680	1.82	593	2.09
		480	2.58	277	4.48
				(346)	(3.58)
cis-$[(H_3N)_2Pt(C_4H_6NO)_2Pt(NH_3)_2]_2^{6+}$ α-pyrrolidone tan	10.82	478	2.59[e]	551	2.25[d]
		415	2.99[e]		

[a] Chain lengths were estimated from crystallographic results as shown in Figure 3. [b] Values were calculated by using the equation ΔE (eV) = $(n^2 - n'^2)(37.60/L^2)$, where n' is the ground state, n is the excited state, and L is in Å. [c] The first two numbers in each group represent $n = 3 \rightarrow n = 4$ and $n = 1 \rightarrow n = 4$ transitions. The numbers in parentheses are for the parity-forbidden $n = 2 \rightarrow n = 4$ transitions in systems having an inversion center. [d] Value for the $n = 3 \rightarrow n = 4$ transition. [e] Reference 12.

geometric changes that play an important role in mediating the solution stability and spectroscopic properties of these compounds.

While the distances and angles within the coordination planes are comparable in all three $(Pt^{2.25})_4$ complexes, **1** displays the largest Pt–Pt distances. The tilt angle (τ) between the Pt1 and Pt2 ligand planes also increases as the Pt–Pt distance increases, with compound **1** having the largest of the three values. The relationship between the tilt angle and the platinum–platinum distance among similar amidate-bridged complexes can be understood on the basis of simple geometric arguments presented elsewhere.[13] The fact that **1** has the largest Pt–Pt distances and τ values of the three platinum blues derives from nonbonded steric interactions between ethylenediamine chelate rings in adjacent coordination planes. This phenomenon is also manifest in the structures of the two α-pyridonate-bridged diplatinum(III) complexes listed in Table V, the Pt–Pt distances being ~0.1 Å longer in the ethylenediamine compounds.

All three platinum blues possess the same zigzag chain structure with a constant Pt1–Pt2–Pt2′ angle of 164.5 ± 0.5°. This angle varies widely among other tetranuclear platinum complexes listed in Table V, with a slight tendency toward linearity with increasing average platinum oxidation state. The tilt angle τ is also found in a fairly narrow range, from 26.4° to 32.1°, for the bridged Pt–Pt planes in $(Pt^{2.25})_4$ complexes. Comparison of tilt angles for related Pt_4 complexes in Table V reveals the expected[13] tendency to lower values with increasing average oxidation state. The other principal geometric feature defining the stereochemistry of the tetranuclear chains, the twist angle ω, shows no clear trend in either the $(Pt^{2.25})_4$ or the other Pt_4 complexes. The ω values for Pt1–Pt2 vary from ca. 6 to 24.3° in the $(Pt^{2.25})_4$ complexes alone. The lack of correlation between ω values for these complexes suggests that they are not closely related to the metal–metal interactions. On the other hand, the increase toward linear Pt1–Pt2–Pt2′ angles as the metal–metal interactions and average platinum oxidation state increase presumably reflects more extensive overlap of d_{z^2} atomic orbitals, which are important components of metal–metal bonding molecular orbitals (vide infra).

Magnetic and ESR Properties. The mixed-valent, $(Pt^{2.25})_4$ character of compounds **1** and **2** was confirmed by their magnetic properties. Temperature-dependent magnetic susceptibility data for solid samples of both complexes gave excellent fits to the Curie–Weiss law. Plots of the experimental and theoretical values of χ vs. T are given in Figures S1 and S2 (supplementary material). The effective magnetic moments of 1.939 (3) μ_B for **1** and 1.891 (3) μ_B for **2** compare favorably with the previously reported value of 1.81 μ_B for **3**[6b] and are consistent with the presence of one unpaired electron per tetranuclear $(Pt^{II})_3Pt^{III}$ unit. From the Curie constants were extracted $\langle g \rangle$ values of 2.24 and 2.19 for **1** and **2**, respectively, in good agreement with the results of electron spin resonance studies of powdered samples of these two complexes at 77 K. Both compounds displayed axial ESR spectra, with $g_\perp = 2.355$, $g_\parallel = 1.97$ and $\langle g \rangle = 2.23$ for **1** and $g_\perp = 2.363$, $g_\parallel = 1.995$, and $\langle g \rangle = 2.240$ for **2**. Single-crystal ESR studies of **3** showed the unpaired electron to reside in a molecular orbital aligned along the mean Pt_4 chain axis.[6b] X-ray photoelectron spectroscopic[28b] and SCF-Xα calculations[16] further revealed the electron to be delocalized over all four platinum atoms.

Electronic Transitions in the Platinum Blues. Free Electron Model for Electronic Spectral Transitions in Platinum Blues. All three structurally characterized platinum blues have two or three intense optical bands between 500 and 800 nm (Table VI). Some aspects of these visible absorption spectra can be understood in terms of one of the simplest quantum mechanical pictures, the free electron model.[32] As just discussed, the unpaired electron

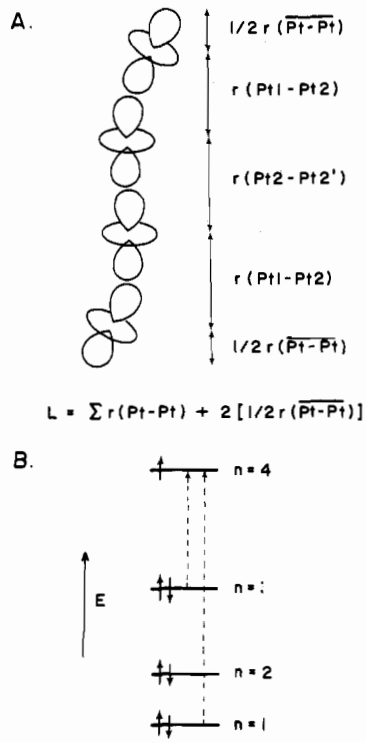

Figure 3. Orbitals (A) and energy levels and allowed transitions (B) in the free electron model for the tetranuclear platinum blues. The length (L) of the chain used to calculate transition energies (Table VI) is estimated as shown in part A where r(Pt–Pt) is the observed bond Pt–Pt distance and $r(\overline{\text{Pt–Pt}})$ is the average Pt–Pt length. See text for further discussion.

in these compounds resides in a d_{z^2}-derived MO delocalized over the four platinum atoms.[28,29] If we assume that this electron is free to move over the entire length of the tetranuclear platinum chain, its energy levels may be calculated from the quantum mechanical results for a one-dimensional particle in a box of length L, $E_n = n^2h^2/8mL^2$, $n = 1, 2, 3, \ldots$. The length corresponds to the sum of four atomic d_{z^2} orbitals described above and is approximated as the sum of the distances between the platinum atoms plus the distance that the terminal d_{z^2} orbitals extend beyond the coordination planes of terminal platinum atoms. This latter distance was estimated by taking half of the average Pt–Pt distance as shown in Figure 3A. Formally, the tetranuclear platinum blues contain one Pt(III) and three Pt(II) atoms, which together contribute seven electrons that are housed in the energy levels in this free electron model. In the ground state these electrons doubly occupy each level through $n = 3$, while the $n = 4$ level is singly occupied. Since the model has an inversion center, only transitions between even and odd states are allowed. The two lowest energy, parity-allowed transitions, then, are $n = 3 \rightarrow n = 4$ and $n = 1 \rightarrow n = 4$ (Figure 3B). The singly occupied $n = 4$ level has three nodes and corresponds directly to the HOMO ($32b_u$) from the SCF–Xα calculation,[16] as will be discussed.

The two lowest transition energies calculated from this model are listed in Table VI, along with the observed absorption maxima for **1**–**3**. The lowest energy calculated transition is in reasonable agreement with the observed values for all three complexes. In addition, the model accurately predicts the shift to higher energy with decreasing metal–metal distance, although the magnitude of the predicted blue shifts is much less than observed. The energies of the next calculated transitions, however, are far from the observed values, suggesting that this band does not arise from an $n = 1 \rightarrow n = 4$ type of transition in the d_{z^2} manifold. Even

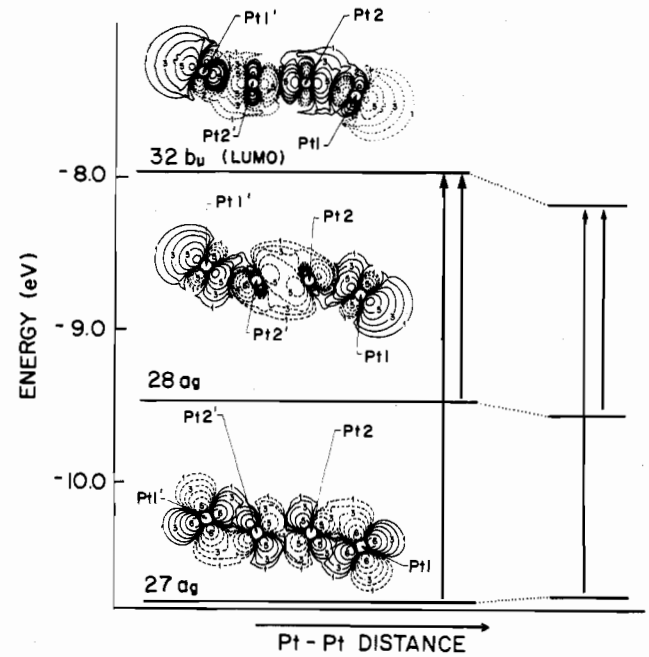

Figure 4. SCF–Xα wave function contour maps and their corresponding energy levels[16] illustrating the effect of increasing the Pt–Pt distance on the electronic transitions responsible for the intense visible bands of the tetranuclear platinum blues. In **3**, the higher energy band at 480 nm results from the $27a_g$ to LUMO transition, while the principal contribution to the lower energy 680-nm band is the $28a_g$ to LUMO transition.[16]

if the parity restriction were lifted, the $n = 2 \rightarrow n = 4$ transition does not match the energy of the next observed band.

Although the absolute and relative energies of the lowest lying intervalence charge-transfer bands of platinum blues **1**–**3** can be rationalized in terms of the free electron model, we caution that this simple picture may not apply in all cases and that not all blue bands in platinum chain complexes will have the same electronic origin. Recently, a blue, trinuclear Pt_2Pd(II,II,III) mixed-valence complex has been prepared with λ_{max} at 608 nm and $\epsilon = 9800$ M^{-1} cm^{-1}.[33] The free electron model predicts a value of 2.99 eV ($\lambda = 415$ nm) for the lowest energy ($n = 2 \rightarrow n = 3$) charge-transfer band of this complex.

SCF–Xα Model for Electronic Spectral Transitions. The results from a recent SCF–Xα calculation[16] for *cis*-diammineplatinum α-pyridone blue substantiate the conclusions drawn from the free electron model for the relative energies of the blue bands in **1**–**3** and provide a detailed picture of the orbitals involved in the transition. Figure 4 depicts the SCF–Xα wave functions for the principal electronic transitions involved in the two intense visible bands of **3**. The 680-nm band has been assigned to three strong intensity transitions to the LUMO $32b_u \downarrow$, predicted to occur in the range 1.5–2.14 eV. The most important contributor is the $28a_g \downarrow$ to LUMO transition shown in the figure. On the basis of changes that occur in the metal–metal interactions as a result of this transition, it has been labeled as a Pt2–Pt2′ $\sigma \rightarrow$ Pt2–Pt2 σ^* transition.

The $28a_g$ and $32b_u$ orbitals correspond to the $n = 3$ and $n = 4$ levels of the free electron model, respectively. The HOMO/LUMO $32b_u$ is antibonding between all adjacent platinum atoms and thus has three nodes. Similarly, the orbital $28a_g$, with Pt2–Pt2′ σ-bonding and Pt1–Pt2 σ-antibonding interactions, is related to the $n = 3$ level, and both contain two nodes.

The only strong intensity transition assigned to the next higher energy (480 nm) band is $27a_g \downarrow \rightarrow 32b_u \downarrow$. Inspection of the $27a_g$ contour map in Figure 4 reveals that this orbital is weakly Pt1–Pt2 π-bonding but is essentially Pt2–Pt2′ nonbonding. Only 18% of the electron density in $27a_g$ is found in the two Pt2 spheres,

(32) This approach is analogous to the use of a free electron model to describe conjugated hydrocarbons as summarized, for example, in: Karplus, M.; Porter, R. N. *Atoms and Molecules: An Introduction for Students of Physical Chemistry*; Benjamin/Cummings: Menlo Park, CA, 1970; p 536.

(33) (a) Lippert, B., private communication. (b) Micklitz, W.; Müller, G.; Riede, J.; Lippert, B. *J. Chem. Soc., Chem. Commun.* **1987**, 76.

whereas 70% is found in the two Pt1 spheres. Again, on the basis of the most important change in metal–metal interactions, the 480-nm transition is labeled Pt1–Pt2 $\pi \rightarrow$ Pt1–Pt2 σ^*.

Clearly, orbital $27a_g$ does not correspond to a level in the pure d_{z^2} manifold used in the free electron model for **3**. The SCF–Xα results thus explain the inability of this simplified model to predict accurately the energy of the 480–532-nm transitions in the platinum blues. In fact, the free electron model $n = 1$ level corresponds to SCF–Xα orbital $23a_g$, which is Pt1–Pt2 and Pt2–Pt2′ σ-bonding.[16] A transition from $23a_g$ to the LUMO is predicted by the SCF–Xα calculation to occur at ca. 5.8 eV (213 nm), while the $n = 1$ to $n = 4$ transition of the free electron model is found at 4.26 eV (291 nm).

Semiquantitative Model for the Effect of Metal–Metal Distances on Visible Transitions in the Platinum Blues. The effect of increasing the Pt–Pt distances on the relative energies of the molecular orbitals involved in the visible transitions of $(Pt^{2.25})_4$ complexes can be deduced by inspecting the bonding character of the SCF–Xα wave functions of **1**. Increasing the internuclear distances raises the energy of an orbital with bonding interactions and lowers the energy of an orbital with antibonding interactions. This analysis is summarized graphically in Figure 4.

The LUMO, $32b_u$, which is antibonding between all pairs of adjacent Pt atoms, is stabilized and moves to lower energy as both outer (Pt1–Pt2) and inner (Pt2–Pt2′) distances increase.

Orbital $28a_g$ has both bonding and antibonding components. The antibonding Pt1–Pt2 interaction is weaker than the corresponding interaction in $32b_u$, owing to a less favorable overlap of the hybrid atomic orbitals. It is also stabilized with increasing Pt1–Pt2 distance, but less so than $32b_u$. The Pt2–Pt2′ bonding interaction in $28a_g$, on the other hand, is destabilized as Pt2–Pt2′ distances increase. Since there are two Pt1–Pt2 interactions for every Pt2–Pt2′ interaction, changes in the former distance should dominate the change in energy. Consequently, the net shift of orbital $28a_g$ is to lower energy, but the magnitude of this shift is smaller than that of $32b_u$ for an equivalent change in Pt-Pt distance.

Weak π-overlap in orbital $27a_g$ can be seen in Figure 4. The effect of increasing Pt–Pt distances on the weak Pt1–Pt2 π-bonding and Pt2–Pt2′ π-bonding interactions of $27a_g$ will be small. The energy of this orbital will therefore increase only slightly, if at all, with Pt–Pt distance.

Several predictions derive from the foregoing analysis of the net changes in orbital energies: (1) both transitions should be shifted to lower energy as the platinum–platinum distances increase; (2) the higher energy transition will be shifted significantly more than the low-energy transition; (3) changes in the Pt1–Pt2 distances have a greater effect than changes in the Pt2–Pt2′ distances. The results for all three $(Pt^{2.25})_4$ complexes are consistent with these semiquantitative predictions.

As the Pt1–Pt2 distances increase by 0.056 (1) Å in going from **3** to **1**, the higher energy band is red-shifted by 0.25 eV. The lower energy transition is also red-shifted, but only by 0.16 eV. Similarly, as the Pt1–Pt2 distance increases by an average of 0.027 (9) Å going from **3** to **2**, the higher energy band is red-shifted by 0.15 eV. In addition to having longer Pt1–Pt2 distances, compound **2** has a slightly shorter Pt2–Pt2′ distance compared with compound **3**. The fact that changes in the Pt2–Pt2′ distance have little effect on the spectroscopic transitions, especially by comparison with Pt1–Pt2 distance alterations, is fully consistent with the foregoing predictions. The additional band at 480 nm in the spectrum of the 1-methyluracil blue (Table VI) cannot be definitively assigned without single-crystal polarized spectroscopy. Several possible transitions could account for this band (see Tables II and V in ref 16) in **2**, which lacks a center of symmetry and should have more intense transitions than **1** or **3**.

As more mixed-valence tetranuclear platinum chain complexes are characterized, these correlations between stereochemistry, electronic structure, and visible spectroscopy can be further developed. Recently, a series of highly colored α-pyrrolidonate Pt_4 complexes were structurally characterized and assigned average platinum oxidation states ranging from 2.14 to 2.50. All but one of these complexes were characterized as "nonstoichiometric" mixtures of $(Pt^{2.0})_4$, $(Pt^{2.25})_4$, and $(Pt^{2.5})_4$ cations, labeled as α-pyrrolidone tan, violet, or green. Although some spectroscopic information is now available for these complexes, it is difficult to interpret their electronic structures in terms of the models presented here for $(Pt^{2.25})_4$ complexes because the metal–metal distances of their stoichiometric components are not known. For the $(Pt^{2.50})_4$ *cis*-diammineplatinum α-pyrrolidone tan, however, application of the free electron model (Table VI) predicts the energy of the $n = 3$ to $n = 4$ transition to be 2.25 eV, compared to the observed value of 2.59 eV. Thus, for this compound the model gives a value 15% lower than the observed one, while for the Pt_4 blues the calculated values were ~20% higher. The difference might possibly be due to electron correlation (pairing) energies which render the $n = 3 \rightarrow n = 4$ transition in the $(Pt^{2.5})_4$ compound energetically more favorable than the corresponding transition in the $(Pt^{2.25})_4$ blues.

Conclusion

The present results for only the second and third crystalline tetranuclear platinum(2.25) blues provide valuable insights into the relationship between stereochemistry and electronic structure. Comparison with other tetranuclear platinum complexes reveals that the Pt1–Pt2–Pt2′ angle and tilt angle (τ) in the blues are limited to a narrow range of values despite changes, in the steric bulk of the nonbridging ligand and the nature of the briding ligand, that modulate the Pt–Pt distances and the twist angles (ω). Of the two or three intense visible absorption bands responsible for the color of these complexes, the one at lowest energy can be explained in terms of a simple free electron model in which an unpaired (d_{z^2}) electron is delocalized in a one-dimensional box corresponding to the length of the tetranuclear platinum chain. The results of a recent SCF–Xα calculation for *cis*-diammineplatinum α-pyridone blue have been used to extend this model to correlate changes in metal–metal distance with shifts in both visible transitions. The trends in the structural and spectroscopic data are unified by this theoretical approach, establishing that the intense colors in $(Pt^{2.25})_4$ blues arise from metal–metal charge-transfer transitions that vary predictably in energy with metal–metal distance.

Acknowledgment. This work was supported by PHS Grant CA 34992 awarded by the National Cancer Institute, DHHS. We thank Drs. W. A. Armstrong and Ch. Pulla Rao for experimental assistance, Professor J. K. Barton for stimulating discussions, Dr. B. Lippert for informing us of his results prior to publication, and Engelhard Industries for a generous loan of K_2PtCl_4 from which the complexes were synthesized. P.K.M. was supported by a grant from the Bristol-Myers Co.

Registry No. **1**, 92127-09-8; **2**, 92220-63-8; **3**, 62782-86-9; $[(en)Pt(C_5H_4NO)_2Pt(en)]_2(NO_3)_4$, 86372-66-9; $[(H_3N)_2Pt(C_5H_5N_2O_2)Pt(NH_3)_2](ClO_4)_5$, 92283-14-2; *cis*-$[Pt(NH_3)_2(H_2O)_2]^{2+}$, 20115-64-4; *cis*-$[Pt(NH_3)_2I_2]$, 15978-93-5; *cis*-$[Pt(NH_3)_2(1\text{-MeU})_2]$, 83350-97-4; Pt, 7440-06-4.

Supplementary Material Available: Tables of thermal parameters for **1** (Table S1) and **2** (Table S3) and hydrogen atom positional parameters for **2** (Table S5) and figures displaying χ_M vs. T plots for **1** (Figure S1) and **2** (Figure S2) (5 pages); tables of structure factors for **1** (Table S2) and **2** (Table S4) (23 pages). Ordering information is given on any current masthead page.